*Original Research*

# Genome-wide Identification, Characterization, and Expression Analysis of *NHX* Genes in *Phaseolus vulgaris* L. under Salt Stress: An *In Silico* Approach

Edinara Maria Barbosa[1] [ID], Jardel de Oliveira[2] [ID], Tiago Benedito dos Santos[2] [ID], Silvia Graciele Hülse de Souza[1],*[ID]

[1]Department of Biotechnology Applied to Agriculture, Universidade Paranaense (UNIPAR), 87502-210 Umuarama, Brazil
[2]Department of Agronomy, Universidade do Oeste Paulista (UNOESTE), 19050-920 Presidente Prudente, Brazil
*Correspondence: silviahulse@prof.unipar.br (Silvia Graciele Hülse de Souza)
Academic Editor: Gustavo Caetano-Anollés

## Abstract

**Background**: Climate change is among the major triggering agents of abiotic stresses (e.g., saline stress), culminating in a vulnerability of common bean production systems. In recent decades, important research has identified and characterized genes that can mitigate the adverse effects caused by salt stress; among them, the $Na^+/H^+$ antiporters (*NHXs*) gene stands out. The *NHX* genes are widely distributed in all organisms and play significant roles in osmotic regulation in plants under salt stress conditions. Genome-wide identification of *NHX* genes has been performed in several plant species but not in *Phaseolus vulgaris* L. **Methods**: This study aimed to identify and characterize *NHX* genes in *P. vulgaris* L. using a genome-wide analysis approach conducted *in silico*. The common bean genome revealed nine putative *PvNHX* genes, and their subcellular localization, phylogenetic relationship, cis-regulatory elements, conserved motifs identification, chromosomal location, expression patterns, and interaction networks were analyzed. **Results**: Promoter analysis suggested that *PvNHX* genes shared hormone-related elements and were light-responsive and stress-responsive. Seven *PvNHX* genes were under the regulation of five microRNA (miRNA) families. RNA-seq analysis revealed that most *PvNHX* genes were expressed in response to salt stress. Currently, the most assertive strategy to confront these adversities is to use the information generated by sequencing plants to identify candidate genes that can be introgressed to improve programs in producing resilient cultures. **Conclusion**: These results can provide valuable information for future studies on the functional mechanism of *PvNHX* genes in common beans in response to salt stress.

**Keywords:** climate change; common bean; expression profile; *NHX* gene; salt tolerance

## 1. Introduction

Global climate change in recent decades has triggered prolonged and severe droughts in many parts of the world. Consequently, irrigation with low-quality water sources was increased, and fertilization practices accelerated soil salinization [1]. Saline stress is more likely to affect areas with increased temperature, lower rainfall, and high evaporation and transpiration rates. Salinity and other abiotic stresses are considered a significant threat to modern agriculture, compromising the growth and development of essential crops [2]. In addition, salinity stress triggers changes in physiological responses and biochemical pathways in plants, decreasing leaf area, photosynthesis, and transpiration [3,4]. Another significant effect is the increased production of reactive oxygen species (ROS) due to the destabilization of cellular homeostasis, causing damage to proteins, DNA, and lipids [5]. When the $Na^+$ and $Cl^-$ contents in the soil are high, the ability of the plant to absorb and transport other mineral nutrients, especially $NO_3^-$, $K^+$, and $Ca_2^+$, declines because these nutrients directly interfere with the pH of the soil [6,7].

Throughout evolution, plants have developed adaptation strategies and mechanisms to overcome high salinity in the soil through specialized channels denominated $Na^+/H^+$ antiporters (NHXs) [5]. Briefly, NHXs feature multifunctions related to salt tolerance, development, cell expansion, growth performance, and disease resistance of plants [8]. NHXs are classified as ubiquitous transmembrane proteins belonging to the monovalent cation/proton antiporter 1 (CPA1) superfamily, whose members are found in prokaryotes and eukaryotes [9]. NHXs have some notable features: homodimers in the cell membrane and conserved regions that can transport $Na^+$ and $H^+$ to 10–12 transmembrane regions in the N terminus [10]. Another important feature of NHX proteins is that they can be classified into three groups according to their cellular location: NHX proteins can be localized in the plasma membrane, vacuole, and endosome [11–13]. Eight NHX members have been identified in *Arabidopsis thaliana*; four genes (*AtNHX1*, *AtNHX2*, *AtNHX3*, and *AtNHX4*) are predicted in the vacuole, two genes (*AtNHX5* and *AtNHX6*) localize in the endosome, and two genes (*AtNHX7* and *AtNHX8*) on the plasma membrane

[9,11,14]. During the evolutionary process, the NHX family maintained highly conserved regions, indicating that this family is essential in the mechanisms involved in the development and survival of organisms [13,15,16].

Subsequent studies have reported the involvement of NHX proteins in salt stress response processes [17–19]. Gaxiola *et al.* [20] first reported the identification of *AtNHX1* in *A. thaliana*. NHXs are vital for plant salt tolerance and preventing $Na^+$ buildup in the cytosol. Vacuolar NHX proteins, such as AtNHX1, sequester $Na^+$ into vacuoles, maintaining osmotic balance and water uptake, while under salt stress, plasma membrane NHX proteins, such as Salt Overly Sensitive 1 (SOS1) (AtNHX7), expel $Na^+$ into the apoplast via the Salt Overly Sensitive (SOS) pathway [20]. Recent progress in next-generation sequencing (NGS) has facilitated the identification of *NHX* genes in many plant species, including *Oryza sativa* [21], *Beta vulgaris* L. [22], *Vitis vinifera* [23], *Triticum aestivum* L. [16], *Canavalia rosea* [24], and *Lonicera japonica* Thunb. [25]. Among the *NHX* genes identified, some successful examples have been identified that mitigated the effect of saline stress [26–33]. In transgenic plants of *Arachis hypogaea* L. transformed with the *AtNHX1* gene, a significant tolerance was observed under saline stress conditions [26]. In another study, it was reported that under saline stress conditions (150 mM NaCl), tomato plants transformed (T1: cv. PED) with the *TaNHX2* gene via *Agrobacterium* mediation showed highly efficient development under such circumstances [27]. Additionally, it is also worth mentioning that physiologically, these plants also showed an increase in the chlorophyll content and the relative water content, further enhancing tolerance in these plants. For example, Yarra and Kirti [28] suggested in another study using *Solanum melongena* L. that *TaNHX2* gene overexpression triggered plant improvements under saline stress (200 mM NaCl). Moreover, an accumulation of proline, improvement in photosynthetic efficiency, and stable water and chlorophyll contents in the leaf were observed in these transformed plants. Studies aimed at transgenic tobacco plants transformed with the *TaNHX1* and *TaNHX3* genes (*Triticum aestivum*) exhibited increased salinity tolerance [29–31]. Indeed, the overexpression of the *NHXs* gene in these studies contributed to plant resistance against saline stress, demonstrating greater efficiency in scavenging ROS and consequently improving the antioxidant activity enzyme [32,33].

The common bean (*Phaseolus vulgaris* L.) stands out among the important agronomic crops. *Phaseolus vulgaris* L. is considered a fundamental food in human nutrition because it is highly nutritious [34]. Meanwhile, despite being cultivated in different environments, the production and development of common beans can be affected by abiotic stresses. Therefore, an urgent need exists to develop new and efficient strategies for breeding abiotic stress tolerance improvement in common beans. The generation and availability of access to the high-quality genome of the common bean [35] provide an unprecedented opportunity to perform a genome-wide identification of essential genes such as *NHX*. Hence, this study identified and comprehensively characterized the number, exon/intron distribution and conserved motifs, chromosomal locations, *cis*-regulatory elements analysis, phylogenetic relationships, and *NHX* gene duplication throughout the *P. vulgaris* L. genome. In addition, tissue-specific and saline-responsive *NHX* gene expression patterns were also observed. This study can enhance the understanding of the *NHX* genes and provide essential information for further functional studies of *NHX* and future molecular breeding of common beans.

## 2. Materials and Methods

### 2.1 Identification of PvNHX Genes in the Common Bean

To identify the *NHX* candidate genes from *P. vulgaris* L., we used the AtNHX protein sequences from *A. thaliana* retrieved from The Arabidopsis Information Resource (TAIR) database (https://www.arabidopsis.org/). Then, these candidates were used as query sequences in the BlastP algorithm (Target type: Proteome) in the Phytozome genome database (https://phytozome-next.jgi.doe.gov/info/Pvulgaris_v2_1/) [36]. The protein, genomic, and CDS (coding sequence) sequences were retrieved for each candidate gene. Briefly, to validate the reliability of these potential candidates, the Pfam database (https://pfam.xfam.org/) [37] was exploited to confirm the identity of each identified *NHX* gene. For nomenclature, the prefix Pv for *P. vulgaris* L. was added, followed by NHX, and numbered according to the gene position on chromosomes 1 to 11, as described in Table 1.

Physicochemical characteristics of the PvNHX putative proteins were evaluated using ExPASy ProtParam online software (http://web.expasy.org/protparam/) [38], including the number of amino acids (aa), theoretical isoelectric point (pI), and theoretical molecular weight (MW). Then, the subcellular localization predictions were performed by the Plant mPLoc server (http://www.csbio.sjtu.edu.cn/bioinf/plant-multi/) [39], and the number of transmembrane domains (TMDs) was identified using the TMHMM server v2 (http://www.cbs.dtu.dk/services/TMHMM/) [40]. Finally, the phosphorylation sites in the PvNHX proteins were predicted using the NetPhos 3.1 Server (https://services.healthtech.dtu.dk/service.php?NetPhos-3.1/) [41].

### 2.2 Gene Structure Analysis and Conserved Motifs in PvNHX Genes

The exon/intron structure organization was performed by accessing the Gene Structure Display Server online tool (GSDS: https://gsds.gao-lab.org) [42]. In addition, the conserved motifs in the PvNHX protein sequences were obtained and analyzed using the online Multiple Expectation Maximization for Motif Elicitation (MEME) tool (https://meme-suite.org/meme/tools/meme) [43], and the parame-

**Table 1. Identification and sequence analysis of the Na$^+$/H$^+$ antiporter (*NHX*) genes in *P. vulgaris* L.**

| *PvHsp* | Phytozome ID | Chromosomal location and strand | Nucleotide CDS (bp) | Length (aa) | MW (kDa) | pl | Subcellular location | Number of predicted TMHs | Amino acids in TMHs |
|---------|--------------|----------------------------------|---------------------|-------------|----------|------|----------------------|--------------------------|---------------------|
| *PvNHX1* | Phvul.001G115000 | Chr01:29357522..29358012 | 375 | 125 | 13.76 | 10.36 | Chloroplast, nucleus. | 0 | 13.77 |
| *PvNHX2* | Phvul.002G185150 | Chr02:34625525..34668002 | 3438 | 1146 | 126.66 | 6.90 | Cell membrane | 12 | 256.73 |
| *PvNHX3* | Phvul.003G089800 | Chr03:22433003..22442132 | 1608 | 536 | 58.78 | 5.49 | Vacuole | 9 | 240.60 |
| *PvNHX4* | Phvul.003G100600 | Chr03:27057886..27061804 | 1641 | 547 | 60.25 | 9.12 | Vacuole | 11 | 233.46 |
| *PvNHX5* | Phvul.006G050200 | Chr06:15480868..15486011 | 1584 | 528 | 59.14 | 7.25 | Vacuole | 10 | 239.91 |
| *PvNHX6* | Phvul.006G097100 | Chr06:20760842..20765235 | 1650 | 550 | 60.88 | 7.71 | Vacuole | 12 | 243.84 |
| *PvNHX7* | Phvul.006G134033 | Chr06:24198038..24209680 | 1605 | 535 | 58.15 | 5.32 | Vacuole | 10 | 238.71 |
| *PvNHX8* | Phvul.007G182200 | Chr07:30229682..30235273 | 1605 | 535 | 59.10 | 6.75 | Vacuole | 11 | 248.47 |
| *PvNHX9* | Phvul.007G184100 | Chr07:30361112..30366673 | 1629 | 543 | 59.66 | 6.92 | Vacuole | 10 | 230.77 |

CDS, coding sequence; MW, molecular weight; TMH, transmembrane helical.

ters were set as follows: the maximum number of identified motifs, 16; minimum width of motif, 6; maximum width of motif, 50.

### 2.3 PvNHX Gene Chromosomal Locations and Duplication Events

The position information for each *PvNHX* gene on the chromosome was obtained from the *P. vulgaris* L. genome database. The physical position of these genes on the chromosome was mapped using MapChart 2.2 software (Wageningen University and Research, Wageningen, Netherlands: https://www.wur.nl/en/show/mapchart.htm) [44]. Then, the synonymous (*Ks*) and non-synonymous (*Ka*) substitution rates of the paralogs and orthologs were further investigated using the *Ka*/*Ks* calculation tool (https://sourceforge.net/projects/kakscalculator2/) [45]. Moreover, the approximate dates of the duplication events were calculated using the formula ($T = Ks/2\lambda$), assuming an average value for the synonymous substitution rate ($\lambda$) of $8.46 \times 10^{-9}$ [35]. Finally, TBtools (v0.655) (https://github.com/CJ-Chen/TBtools) was used to represent the duplication events graphically.

### 2.4 Phylogenetic Analysi

Multiple sequence alignment of proteins was performed using T-Coffee with the default parameters. Phylogenetic analysis was performed using the MEGA X program (Molecular Evolutionary Genetics Analysis [46], with the maximum likelihood (ML) method and branch support values with a bootstrap test of 1000 replicates to understand the evolutionary relationship between *P. vulgaris* L. and other plants (*A. thaliana*, *Glycine max*, *Oryza sativa*, *Medicago truncatula*, *Vitis vinifera*, and *Zea mays*). The IDs of proteins used in the phylogenetic analysis are listed in **Supplementary Table 1**.

### 2.5 Synteny Analysis

To compare the *NHX* genes and establish orthologous relationships among *P. vulgaris* L. and *A. thaliana*, *P. vulgaris* L. and *O. sativa*, and *P. vulgaris* L. and *G. max*, we first performed reciprocal BlastP. The hit threshold values were set as E-value $<1 \times 10^{-50}$, score $>200$, minimum 80% coverage, and 70% identity [47]. The TBtools (v0.655) (https://github.com/CJ-Chen/TBtools) was used to represent the duplication events graphically.

### 2.6 Promoter Sequence Analysis

For this analysis, the genomic sequences of the 5′ upstream regions (1.5 kb DNA sequence) of the initiation codon ATG in the *PvNHX* genes were downloaded from the Phytozome database and then submitted to the PlantCARE tool (http://bioinformatics.psb.ugent.be/webtools/plantcare/html/) [48] to predict the *cis*-regulatory elements in the promoter regions.

### 2.7 The miRNA Target Sites Analysis

The *PvNHX* CDS sequences and microRNA (miRNA) sequences of *P. vulgaris* L., previously obtained from PmiREN (Plant miRNA Encyclopedia: https://www.pmiren.com/), were used to predict targeted miRNAs using the psRNATarget server (https://www.zhaolab.org/psRNATarget/) using default parameters.

### 2.8 Protein Interaction Analysis and 3D Prediction

Interacting protein networks were predicted using the STRING tool (https://string-db.org/) based on a model plant, *A. thaliana*. Subsequently, all PvNHX amino acid sequences were submitted to Phyre2 (http://www.sbg.bio.ic.ac.uk/~phyre2/) [49], and 3D protein structure models for *PvNHX* genes were predicted using homology modeling in the default mode.

### 2.9 In Silico Expression Analysis

The Phytozome database (https://phytozome-next.jgi.doe.gov/info/Pvulgaris_v2_1) was used to retrieve the Illumina RNA-seq datasets from various tissues and developmental stages of *P. vulgaris* L. We examined the expression patterns of the *PvNHX* genes in ten distinct developmental stages, including nodules, root 10, root 19, stem 10, stem 19, young pods, green mature buds, leaves, young trifoliate, flower buds, and flowers. We used RNA-seq transcriptomes and the associated FPKM (fragments per kilobase of transcript per million mapped reads) values. Next, the FPKM values were $\log_2$ transformed, and the heatmap was built using the online program Clustvis (http://biit.cs.ut.ee/clustvis/) [50].

### 2.10 In Silico Expression Analysis of PvNHX Genes under Salt Stress

We employed the RNA-seq transcriptome database for datasets from two common bean varieties, the Ispir (salt-tolerant) and TR43477 (salt susceptible), to identify the salt-induced expression profile [51]. Illumina RNA-seq data were obtained from the Sequence Read Archive (SRA) data library in the National Center for Biotechnology Information (NCBI) database. These data are available under the accession code 'SRP277207'. In addition, the online program Clustvis was used to show the differential expression of the two conditions/genotypes (https://biit.cs.ut.ee/clustvis/) [50].

## 3. Results

### 3.1 Genome-Wide Identification of NHX Genes in P. vulgaris L.

In the current study, nine *PvNHX* genes with the NHX domain were identified in the common bean genome; for convenience, these were named *PvNHX1* to *9* according to their chromosomal positioning (Table 1). Detailed information on these *PvNHX* genes can be found in Table 1.

PvNHX proteins exhibited significant variation in size, with PvNHX1 being the shortest at 125 amino acids, while PvNHX2 was the longest, comprising 1146 amino acids. The molecular weight of these proteins ranged from 13.76 kDa (PvNHX1) to 126.66 kDa (PvNHX2). Subsequently, we predicted the isoelectric points (pIs) of the PvNHX proteins, which also presented significant differences. The pI of PvNHX7 was 5.32, and PvNHX1 was 10.36, the smallest and largest pIs in the *PvNHX* gene, respectively (Table 1).

The subcellular localization prediction showed eight PvNHX proteins were situated in the vacuolar (Vac) region, while one protein (PvNHX2) was found in the plasma membrane (PM) (Table 1). The prediction of TMs indicates that PvNHX proteins possess multiple transmembrane regions, a characteristic typical of membrane-bound ion transporters. TMD data analysis identified that PvNHX1 has no domain, while PvNHX2 and PvNHX6 have 12 TMDs each (Table 1; **Supplementary Fig. 1**). These results demonstrate that the most identified PvNHX presents the arranged membrane-bound and structural diversity among the *PvNHX* genes. In addition, PvNHX phosphorylation sites varied in number (**Supplementary Table 2**). These sites ranged from 8 to 86, 6 to 34, and 0 to 9 for serine, threonine, and tyrosine sites, respectively.

### 3.2 Gene Structure Analysis and Conserved Motifs in PvNHX Genes

Understanding the organization of exon/intron structures is very important because it can reveal valuable insights into the evolutionary relationships of specific genes. For example, an analysis conducted *in silico* showed that the number of exons in the *P. vulgaris* L. *PvNHX* genes varied from 1 (*PvNHX1*) to 23 (*PvNHX2*), respectively (Fig. 1a). The conserved motif composition was analyzed to assess the structural characteristics and diversity of the common bean PvNHXs proteins. The phylogenetic tree and conserved motifs showed characteristics of the NHX gene family (Fig. 1b). The information on these motifs predicted using the MEME tool indicated that the motifs 1, 2, 3, 6, 8, and 9 shared a common Pfam domain (CL0064), a conserved domain in the sodium/hydrogen exchanger family (Fig. 1b). Additionally, the amiloride-binding site (FFIYLLPPI), a characteristic of NHX proteins, was detected in motif 2; most proteins localized on vacuoles and endosomes. We found the binding site of amiloride in most members, but it was absent in two members (PvNHX1 and PvNHX2) (Fig. 1b).

### 3.3 Chromosomal Location and Gene Duplication

Chromosomal location analysis revealed that *PvNHX* genes were mapped on chromosomes 1, 2, 3, 6, and 7 (Fig. 2a). Chromosome 6 contains the highest number, with three genes, while chromosomes 2, 3, and 7 each have two. Chromosome 1 harbors a single gene. A collinearity analysis was conducted to explore gene duplication events among the *PvNHX* genes. Five duplication events were identified within the *P. vulgaris* L. genome (Fig. 2a; Table 2), all occurring through segmental duplication. These findings indicate that segmental duplication was key in expanding the *PvNHX* gene family throughout the common bean genome.

### 3.4 Phylogenetic Analysis, Classification, and Synteny Analysis of PvNHX Genes

To clarify the evolutionary relationships among NHX proteins, a phylogenetic tree was constructed using 60 amino acid sequences from various plant species, including *P. vulgaris* L., *A. thaliana*, *G. max*, *M. truncatula*, *P. trichocarpa*, *V. vinifera*, and *O. sativa*. The results, presented in Fig. 3, revealed that the PvNHX proteins clustered into three distinct clades based on sequence similarity and subcellular localization: endosomal (Endo), plasma membrane (PM), and vacuolar membrane (Vac) (Fig. 3).

Additionally, a synteny analysis was performed to compare *NHX* genes in *P. vulgaris* L. with those from one monocot species (*O. sativa*; Fig. 4a) and two dicot species (*A. thaliana* and *G. max*; Fig. 4b,c). *G. max* was included due to its close relationship with the common bean. This analysis identified 14 syntenic gene pairs between *P. vulgaris* L. and *A. thaliana* and six pairs between *P. vulgaris* L. and *O. sativa* (Fig. 4; **Supplementary Table 3**). Notably, the *AtNHX7* and *AtNHX8* genes in *A. thaliana*, as well as *OsNHX4*, *OsNHX5*, *OsNHX6*, and *OsNHX7* in *O. sativa*, exhibited no synteny with the *P. vulgaris* L. genome. Conversely, the *PvNHX2* and *PvNHX8* genes were found to be species-specific to *P. vulgaris* L.

All *NHX* genes in *P. vulgaris* L. showed synteny with their corresponding *NHX* genes in *G. max*, reflecting a high degree of genomic conservation between these species. Furthermore, several *P. vulgaris* L. genes exhibited multiple orthologous relationships with *G. max* genes, with 25 *NHX* gene pairs identified. These included 6 *PvNHX* genes and 9 *GmNHX* genes, illustrating the complexity of gene duplication and conservation events between these species.

### 3.5 Promoter Cis-acting Element Analysis of PvNHX Genes

Subsequently, we further analyzed the *cis*-regulatory elements in the promoter regions of *PvNHX* genes. The promoter sequence analysis of the *PvNHX* genes revealed elements related to numerous processes and could be classified into four categories (Fig. 5): elements related to the hormone-responsive (ABRE, abscisic acid; TCA-element, salicylic acid; TGACG-motif, MeJA reactivity; 43 in total), light-responsive (Box4, GATA-motif, G-box; 113 in total), growth and development (circadian; one in total), and stress-responsive (MBS, MYC, MYB, TC-rich-repeats, LTR; 78 in total). The predominance of light-responsive elements in the PvNHX sequences (such as Box4, GATA box, GT1 box, G-box, and G-box motifs) suggest their involvement in photoperiodic and photo-morphogenetic responses
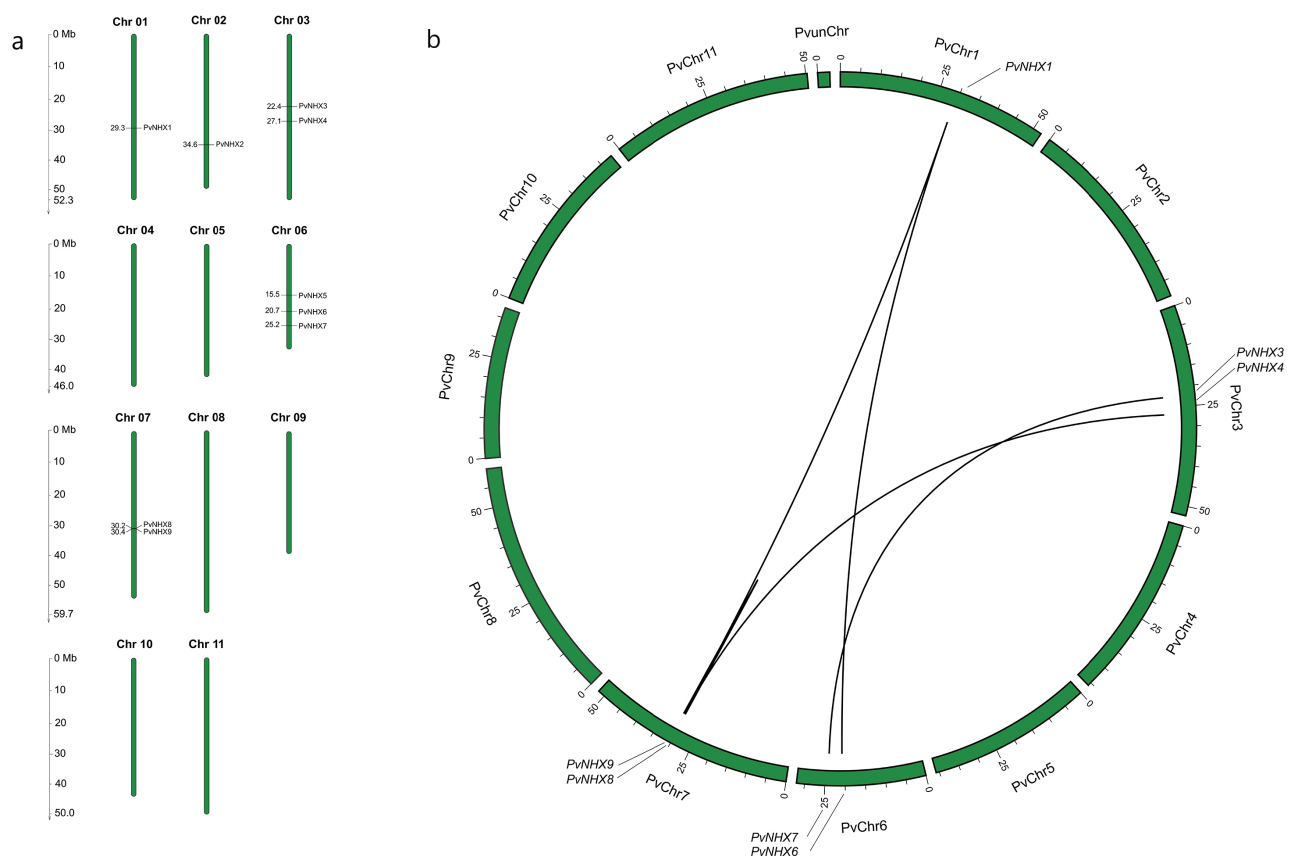
**Fig. 1.** *PvNHX* genes from *Phaseolus vulgaris* L. were analyzed based on their phylogenetic relationships. (a) The exon/intron structural patterns in the *PvNHX* genes were illustrated; yellow rectangles represent exons, gray lines indicate introns, and blue rectangles denote untranslated regions (UTRs). (b) A schematic diagram of the sixteen conserved motifs in the PvNHX proteins was constructed, and motif prediction was performed using the MEME tool. Each motif is represented by numbered boxes of different colors, corresponding to distinct motifs.



**Fig. 2.** Schematic representation of the chromosomal distribution and duplication events of the *PvNHX* genes in the common bean. (a) Chromosomal mapping of *PvNHX* genes across the eleven chromosomes in *P. vulgaris* L. Chromosome numbers and their sizes (in Mb) are displayed at the top of each bar, with the vertical scale denoting chromosome lengths. (b) Duplication events among the *PvNHX* genes in the common bean genome. Black lines within the circular diagram indicate segmentally duplicated genes (Table 2).
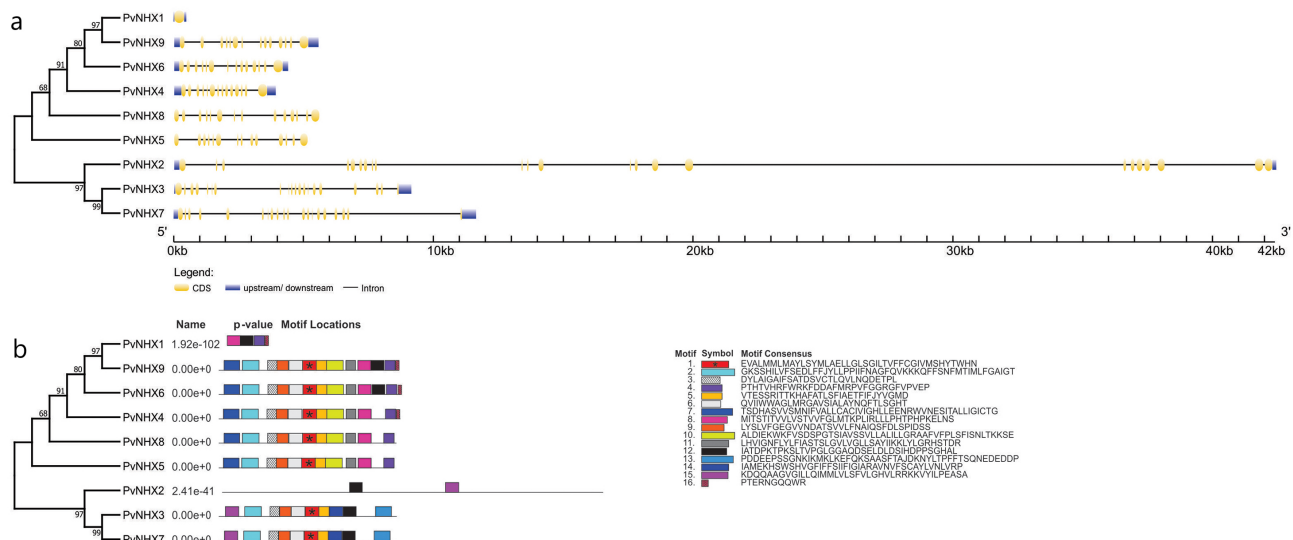
**Table 2. Duplication dates of paralogous gene pairs within the *P. vulgaris* L. *PvNHX* gene family.**

| Paralogous pairs | Chromosomal location | Duplication event | *Ka* | *Ks* | *Ka/Ks* | Date mya | Purifying selection |
|---|---|---|---|---|---|---|---|
| *PvNHX1/PvNHX6* | Chr01/Chr06 | Segmental | 0.30 | 0.25 | 1.21 | 29.87 | No |
| *PvNHX1/PvNHX9* | Chr01/Chr07 | Segmental | 0.02 | 0.03 | 0.63 | 3.66 | Yes |
| *PvNHX3/PvNHX7* | Chr03/Chr06 | Segmental | 0.18 | 0.71 | 0.25 | 84.18 | Yes |
| *PvNHX4/PvNHX9* | Chr03/Chr07 | Segmental | 0.28 | 0.53 | 0.53 | 63.16 | Yes |
| *PvNHX6/PvNHX9* | Chr06/Chr07 | Segmental | 0.19 | 0.28 | 0.68 | 32.61 | Yes |

The parameters include Ka (non-synonymous substitution rate per non-synonymous site), Ks (synonymous substitution rate per synonymous site), Ka/Ks ratio (indicating the selective pressure acting on the genes), and the estimated time of duplication (mya, million years ago).
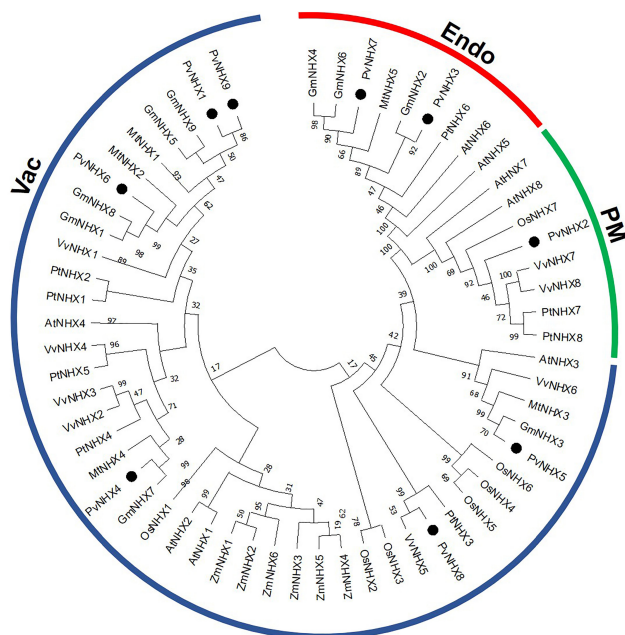


**Fig. 3. A phylogenetic tree of NHX proteins was constructed using the maximum likelihood (ML) method with 1000 bootstrap replicates.** Tree includes NHX proteins from *O. sativa* (Os), *Zea mays* (Zm), *A. thaliana* (At), *V. vinifera* (Vv), *P. trichocarpa* (Pt), *M. truncatula* (Mt), *G. max* (Gm), and *P. vulgaris* L. (Pv). Different colored arcs represent the alternative clades, while black circles highlight the NHX proteins specific to the common bean. Endo, endosomal; PM, plasma membrane; Vac, vacuolar membrane.

(Fig. 5). Interestingly, only one *cis*-regulatory element associated with the biological clock (circadian motifs—PvNHX9) was identified. Among the elements identified, the most abundant in PvNHX involved water and drought response elements (MYB: CAACCA/TAAC/TAACTG; MYC: CAATTG/TCTCTTA/TCTCTTA) (Fig. 5).

### 3.6 Prediction of miRNA Targeting PvNHX

We conducted an analysis to identify miRNAs targeting *PvNHX* genes and predict their binding sites to determine whether miRNAs regulate these genes. It is well established that miRNA-mediated regulation plays a key role in plant stress responses. Those findings revealed that five miRNA families target seven *PvNHX* genes (**Supplementary Table 4**). Notably, five of these genes (*PvNHX2*, *PvNHX4*, *PvNHX5*, *PvNHX8*, and *PvNHX9*) are likely targeted by umiRN2588, representing 50% of the *PvNHX* genes in the common bean.

Most *PvNHX* genes contained target sites for a single miRNA, except for *PvNHX2* and *PvNHX9*, which were targeted by two miRNAs each (*PvNHX2* by PvumiR395 and PvumiRN2588, and *PvNHX9* by PvumiRN2588 and PvumiRN2597). All identified transcripts were degraded through cleavage (**Supplementary Table 4**).

### 3.7 Analysis of Interaction Networks and Three-Dimensional Protein Sequence of NHX

A protein–protein interaction (PPI) network was constructed using the STRING online tool to investigate the functions, signal transduction pathways, and metabolic processes involving NHX proteins (Fig. 6). The PvNHX1, 4, 6, 7, and 9 proteins were found to share several putative interactive partners, including calcineurin B-like (CBL) 1, salt overly sensitive (SOS) 1, SOS2, SOS3, vacuolar pyrophosphatase (AVP) 1, high affinity $K^+$-transporter (HKT) 1, and high-affinity $K^+$ (HAK) 5.

The predicted 3D structural models of the PvNHX proteins from *P. vulgaris* L. (**Supplementary Fig. 2**) revealed that all models contained highly conserved alpha helices (highlighted in pink) and random coils (highlighted in blue). Moreover, the 3D structures of the representative PvNHX proteins from the common bean demonstrated that 95.9–100% of the amino acid sequences were modeled with high confidence (**Supplementary Fig. 2**). Notably, most of these proteins shared the same c7dsvA model, suggesting that their tertiary structures are highly similar.

### 3.8 Expression Pattern of PvNHX Genes in Different Tissues and Different Developmental Stages Using RNA-seq Data

The expression patterns of nine *PvNHX* genes were investigated in different *P. vulgaris* L. tissues based on RNA-seq datasets (FPKM). A heatmap was generated to display the expression pattern of the *PvNHX* genes (Fig. 7). In particular, expression of the *PvNHX7* and *PvNHX9* genes was
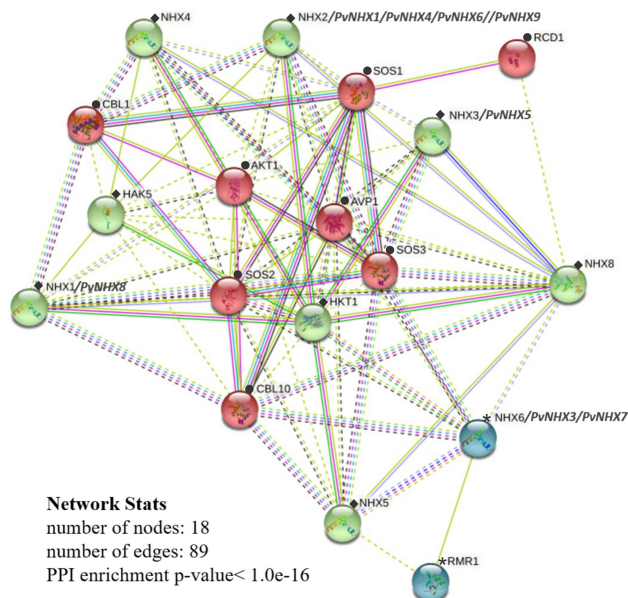
| Genes | TGACG-motif | TCA-element | TGA-element | CGTCA-motif | ABRE | GARE-motif | P-box | ERE | AE-box | Box4 | MRE | ACE | Box II | GATA-motif | Gap-box | I-Box | 3-AF1 binding site | G-box | G-Box | GA-motif | TCT-motif | GT1-motif | TCCC-motif | chs-CMA1a | chs-CMA2a | Circadian | ARE | W box | MBS | MYC | MYB | TC-rich-repeats | LTR |
|---|---|---|---|---|---|---|---|---|---|---|---|---|---|---|---|---|---|---|---|---|---|---|---|---|---|---|---|---|---|---|---|---|---|
| *PvNHX1* | 0 | 0 | 0 | 0 | 3 | 0 | 1 | 0 | 3 | 1 | 0 | 0 | 0 | 2 | 1 | 1 | 0 | 1 | 2 | 1 | 1 | 0 | 0 | 0 | 0 | 0 | 5 | 1 | 0 | 5 | 2 | 0 | 0 |
| *PvNHX2* | 0 | 0 | 0 | 0 | 1 | 0 | 0 | 3 | 1 | 2 | 0 | 0 | 0 | 1 | 0 | 2 | 0 | 1 | 4 | 0 | 1 | 0 | 2 | 0 | 0 | 0 | 0 | 0 | 2 | 2 | 2 | 1 | 0 |
| *PvNHX3* | 0 | 0 | 0 | 0 | 8 | 0 | 0 | 0 | 0 | 3 | 0 | 0 | 0 | 0 | 0 | 1 | 1 | 9 | 3 | 0 | 1 | 1 | 0 | 0 | 1 | 0 | 1 | 2 | 0 | 5 | 5 | 1 | 0 |
| *PvNHX4* | 0 | 1 | 0 | 0 | 0 | 0 | 0 | 0 | 0 | 1 | 1 | 0 | 0 | 1 | 0 | 0 | 0 | 1 | 0 | 1 | 0 | 0 | 1 | 0 | 0 | 0 | 0 | 0 | 1 | 5 | 1 | 1 | 0 |
| *PvNHX5* | 0 | 0 | 0 | 0 | 2 | 0 | 0 | 0 | 1 | 8 | 0 | 0 | 0 | 0 | 0 | 0 | 0 | 1 | 2 | 0 | 0 | 1 | 0 | 0 | 0 | 0 | 2 | 0 | 0 | 1 | 2 | 1 | 0 |
| *PvNHX6* | 0 | 0 | 1 | 0 | 7 | 0 | 0 | 0 | 0 | 4 | 1 | 0 | 0 | 2 | 0 | 0 | 0 | 5 | 2 | 0 | 2 | 0 | 1 | 0 | 0 | 0 | 0 | 0 | 0 | 3 | 1 | 1 | 1 |
| *PvNHX7* | 0 | 1 | 0 | 0 | 1 | 0 | 0 | 0 | 0 | 3 | 0 | 0 | 1 | 2 | 0 | 0 | 0 | 1 | 0 | 0 | 0 | 0 | 0 | 0 | 0 | 0 | 0 | 3 | 3 | 0 | 0 | 0 | 0 |
| *PvNHX8* | 1 | 0 | 0 | 1 | 3 | 0 | 0 | 0 | 0 | 2 | 1 | 0 | 0 | 1 | 0 | 0 | 0 | 1 | 2 | 0 | 1 | 1 | 1 | 0 | 0 | 0 | 3 | 0 | 1 | 3 | 1 | 0 | 0 |
| *PvNHX9* | 1 | 1 | 0 | 1 | 5 | 1 | 0 | 0 | 0 | 5 | 2 | 1 | 0 | 0 | 0 | 0 | 0 | 3 | 3 | 0 | 0 | 0 | 0 | 1 | 0 | 1 | 1 | 0 | 1 | 1 | 6 | 0 | 1 |

Element function groupings — Hormone responsive: TGACG-motif, TCA-element, TGA-element, CGTCA-motif, ABRE, GARE-motif, P-box, ERE. Light responsive: AE-box, Box4, MRE, ACE, Box II, GATA-motif, Gap-box, I-Box, 3-AF1 binding site, G-box, G-Box, GA-motif, TCT-motif, GT1-motif, TCCC-motif, chs-CMA1a, chs-CMA2a. Growth and development: Circadian. Stress responsive: ARE, W box, MBS, MYC, MYB, TC-rich-repeats, LTR.

Color scale legend: 0, 1, 2, 3, 4, 5, 6, 7, 8, 9.

**Fig. 5. *Cis*-regulatory elements detected 1500 bp upstream of the *PvNHX* genes involved in different responses.**

higher than other genes in most analyzed tissues. By contrast, the *PvNHX1*, *PvNHX2*, and *PvNHX6* genes had lower expression levels than others. For example, the *PvNHX2* and *PvNHX6* genes showed low expression in leaves, root 19, and stem 19, while *PvNHX1* was less expressed in flower buds, flowers, and young pods (Fig. 7a). For the other genes, relatively low or moderately low in all analyzed tissues are exhibited by an expression pattern. The transcriptional profiling of *PvNHX* genes resulted in the separation of tissues into three distinct groups (I, II, and III) (Fig. 7b). Group I exhibited moderate expression in tissues associated with the reproductive stages, including mature green pods, flowers, flower buds, and young pods. Group II showed moderate expression in leaves and young trifoli-

ates. Group III, which included stem 10, stem 19, nodules, root 10, and root 19, exhibited high expression levels of most *PvNHX* genes in these tissues (Fig. 7b).

*3.9 Expression Patterns of PvNHX Genes in P. vulgaris L. under Salt Stress*

In this study, RNA-seq data generated by Niron *et al.* [51] were analyzed to investigate the responses of *PvNHX* genes to salt stress in two common bean varieties: Ispir (salt-tolerant) and TR43477 (salt-susceptible). *PvNHX* genes were differentially expressed in both leaf and root tissues under salt stress conditions for both cultivars (Fig. 8A,B). All *PvNHX* genes showed higher expression levels in root tissues under salt stress in the TR43477 culti-

**Fig. 6. The protein–protein interaction networks of the *PvNHX* genes in *P. vulgaris* L. according to the orthologs in *A. thaliana*.** The STRING tool was used to predict the entire network. CBL1, calcineurin B-like; PPI, protein–protein interaction; HAK, high-affinity $K^+$; AKT, low-affinity $K^+$ transporter; SOS, salt overly sensitive; HKT, high affinity $K^+$-transporter; AVP, vacuolar $H^+$-pyrophosphatase pump; RCD, radical-induced cell death protein; RMR, reserve mobilization rate.

var (Fig. 8A). Notably, significant expression changes were particularly evident for the *PvNHX2, 5, 7*, and *9* genes in root tissues under salt stress, compared with the salt-tolerant Ispir cultivar (Fig. 8A). Roots, being the first tissues exposed to salinity, exhibited a notably higher induction of *PvNHX* gene expressions under these conditions.

## 4. Discussion

Different strategies for acquiring salinity tolerance have been developed during the evolution of plants; however, these all involve a complex mechanism linked to the physiology and expression of certain genes [13,52]. The bioinformatics tools allied with genomics can identify new genes and metabolic pathways that are key resources for improving adaptability, for example, of common bean crops to the present and future climate change scenarios. Recently, the *NHX* genes were noted in plants to encode important membrane transporters involved in the development and subsequent tolerance to salt stress [8]. In this study, bioinformatics automatically identified nine *PvNHX* genes (*PvNHX1–9*) in the *P. vulgaris* L. genome. With the advent of the NGS, *NHX* gene members have been identified in many species, including eight in *A. thaliana* [20], seven in *Morus atropurpurea* [53] and *O. sativa* subsp. Indica [54], nine in *Camellia sinensis* [55], and ten in *Punica granatum* L. [18], among others. Thus, a difference can be observed in
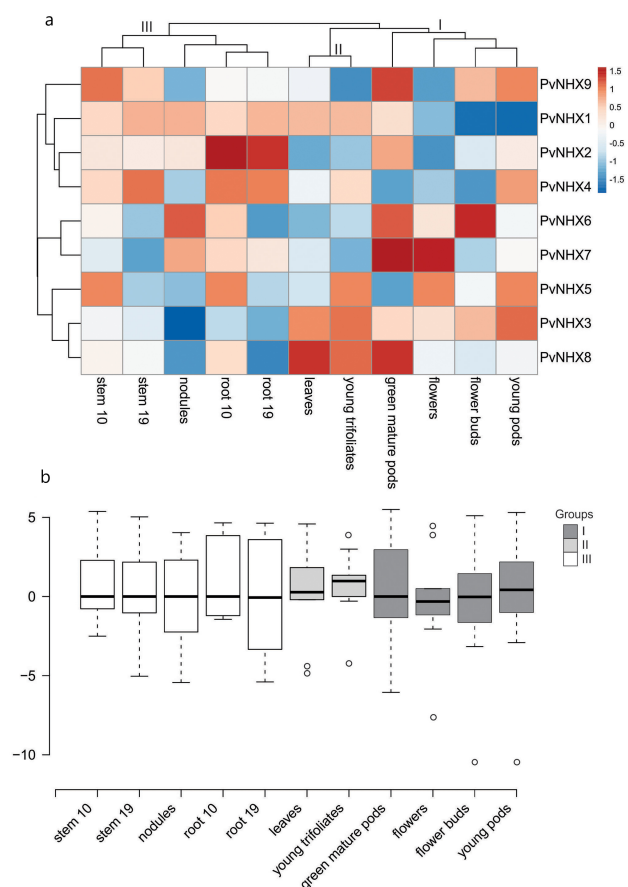


**Fig. 7. Gene expression profiles of *PvNHX* genes in different *P. vulgaris* L. tissues.** (a) Heatmap illustrating the expression levels of *PvNHX* genes across various tissues of *P. vulgaris* L. The color gradient represents normalized expression values. (b) Box plot displaying the distribution of *PvNHX* gene expression across different tissues. The boxes represent the interquartile range (IQR), the horizontal lines inside the boxes indicate the median expression values and the whiskers extend to the minimum and maximum expression levels, excluding outliers.

the number of these genes compared to other plant species, suggesting that duplication and loss of specific *NHX* genes have played an essential role in the evolutionary process.

Previous investigations demonstrated that $Na^+/H^+$ exchangers may be categorized into two primary types—SOS (salt overlay sensitive) and NHX—according to the protein's subcellular location (reviewed by Ayadi *et al.* [56]). The intracellular NHX class can be found in the tonoplast or endosomal compartments and plays crucial functions in response to saline stress. Consequently, we hypothesize that comprehending the subcellular localization of the protein may assist us in deducing the biological function of the PvNHX proteins (Table 1). Moreover, these proteins are primarily situated in the vacuole, chloroplast, nucleus, and cell membrane of common beans, suggesting a role in eliminating harmful chemicals from cells, such as removing Na+/K+ under unfavorable saline circumstances.
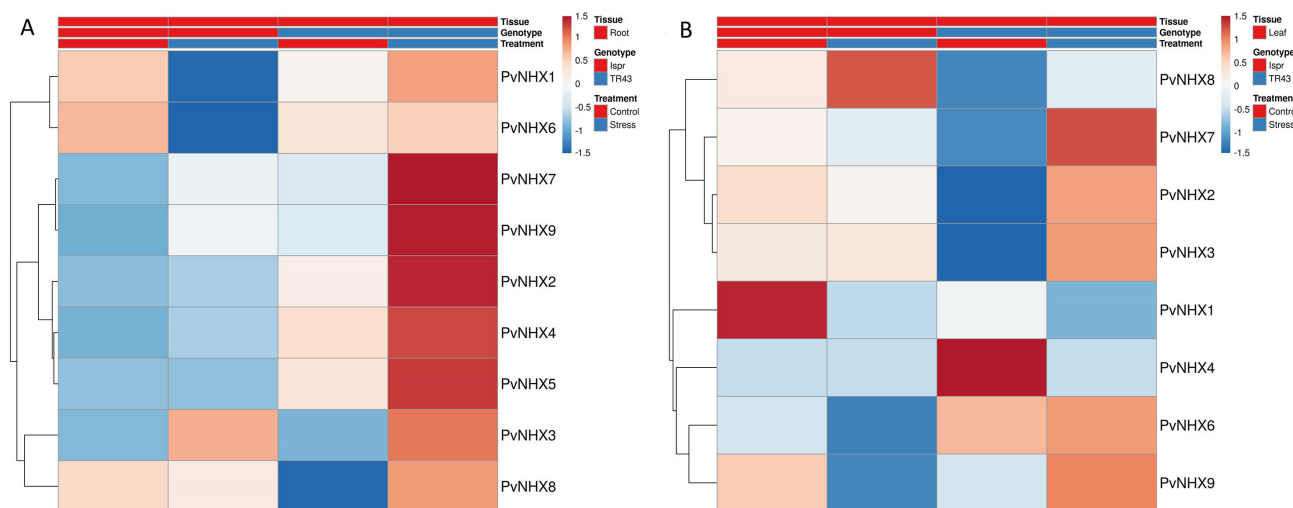
**Fig. 8. Heatmap comparing two bean types (Ispir and TR43477) subjected to salt stress.** (A) Expression profile of *PvNHX* genes in root tissues. (B) Expression profile of *PvNHX* genes in foliar tissues.

It has been previously revealed that all known members of *A. thaliana* are also situated in the vacuole [57,58].

Examining the exon–intron structure revealed that the structures of nine *PvNHX* genes are diverse, with variable numbers of exons and introns, indicating pivotal evolutionary changes within the *P. vulgaris* genome (Fig. 1). *PvNHX1* lacks introns, whereas the remaining eight *PvNHXs* contain a greater number of introns. It is speculated that *PvNHX1* facilitates rapid transcriptional activity in plant development or response to unfavorable environmental conditions [59]. Meanwhile, the number of introns/exons can affect gene transcription levels, whereby genes with fewer introns/exons are expressed faster [60,61]. Additionally, we discovered that *PvNHX1, 6,* and *9* (paralog pairs; 1–6, 1–9) have fewer introns, indicating that these PVNHX proteins in common beans have recently evolved with fewer introns (Fig. 1; Table 2). This corroborates that the number of introns has decreased with time, implying that more recently developed, newer proteins have fewer introns than more ancient ones [62].

Furthermore, similar results were obtained in other plant species, such as *M. atropurpurea* [53] and *P. trichocarpa* [63], revealing that the *NHX* genes are highly conserved in plants, possibly related to their similar functions. Additionally, these nine PvNHX proteins presented the highly conserved amiloride binding domain (FFI/LY/FLLPPI motif; Fig. 1b). Thus, following this rationale, similar results were observed in *P. trichocarpa* [63], *V. vinifera* [23], and *P. granatum* [18]. This implied that the motif (FFI/LY/FLLPPI) in the transmembrane region of PvNHX in the common bean is sensitive to the Na$^+$ of the substrate.

The findings on the chromosomal structure and duplication analysis of the common bean suggest that the majority of *PvNHX* genes are located on distinct chromosomes and do not adhere to a singular pattern (Fig. 2). Gene duplication is arguably crucial for the expansion of gene families and the diversification of their functions [64]. Throughout plant evolution, mechanisms such as segmental duplication, tandem duplication, and transposition events contribute to the growth of gene families [65]. Duplication analysis indicated that the *PvNHX* genes were associated with syntenic blocks (Fig. 2), suggesting that segmental duplication events significantly contribute to the expansion of *PvNHX* in common beans. The *Ka/Ks* ratio values for the *PvNHX* gene pairs varied from 0.25 to 1.21 (Table 2). Various selection categories for duplicated genes are indicated by the *Ka/Ks* ratio, wherein *Ka/Ks >1* signifies positive selection, *Ka/Ks = 1* indicates neutral evolution, and *Ka/Ks <1* represents negative selection [66]. The four pairs of paralogous genes had *Ka/Ks* ratios below 1. This discovery indicates that negative selection pressure influenced most *PvNHX* genes.

In the present study, the phylogenetic tree was constructed to determine the evolutionary relationship between the *PvNHX* genes in *P. vulgaris* L., *O. sativa*, *Z. mays*, *A. thaliana*, *V. vinifera*, *P. trichocarpa*, *M. truncatula*, and *G. max* (Fig. 3). As per previous reports, these results corroborate the grouping of NHX sequences into three distinct clades [22,67,68]. The PvNHX protein sequences were categorized as follows: the PvNHX2 sequences were in the plasma membrane clade. The PvNHX1, PvNHX3, PvNHX4, PvNHX5, PvNHX6, PvNHX7, PvNHX8, and PvNHX9 sequences were in the plasma membrane clade (Fig. 3). Meanwhile, as shown in phylogenetic tree analysis, no NHX proteins were observed in the endosome clade. These results were similarly observed in *G. max* [69]. Furthermore, this result suggests that the nine PvNHX proteins have an evolutionary relationship with other dicot and monocot plants and may have similar functions as their or-

thologs. Additionally, based on the phylogenetic analysis, the group Vac contains more *PvNHX* genes. In this sense, we suggested that these genes were the most conserved during the evolutionary process.

Significant orthologous relationships between the common bean and soybean can be attributed to their evolutionary histories, i.e., *P. vulgaris* L. and *G. max* diverged from a common ancestor. Moreover, these bean variants underwent a whole-genome duplication (WGD) event around 56.5 million years ago, subsequently diverging from each other around 19.2 million years ago [35]. In evolutionary terms, *G. max* underwent an independent WGD around 10 million years ago. No association has been shown for the *PvNHX2* and *PvNHX8* genes in *P. vulgaris* L. and *A. thaliana*, *O. sativa*, or *G. max*, indicating that these genes may have emerged post-divergence of these species (Fig. 4; **Supplementary Table 3**). These genes were only identified in the *P. vulgaris* L. genome, and we suggest that they played an essential role in the evolution of *P. vulgaris* L. Conversely, the *PvNHX4*, *PvNHX6*, and *PvNHX9* genes, together with their orthologues, are found in every examined species. This suggests these genes originated from the same ancestor before separating eudicots and monocots. Furthermore, these genes are related to genes found in *O. sativa*, *A. thaliana*, and *G. max*. Overall, these findings imply that these genes may have a crucial adaptive function in salt-stress conditions.

A unique promoter region regulates each gene in plants. Promoters are non-protein coding regions in genes located upstream of the transcription start site (TSS). Promoters exhibit conserved DNA elements that, along with transcription factors, are essential regulators of gene expression suppression or activation in different tissues, organs, or according to various stages of plant development [70]. As already mentioned, putative *cis*-acting elements related to light response, hormones, stress, and development were identified in the promoter regions of *PvNHX* genes in the common bean (Fig. 5). These elements are also a strong indication that biotic and abiotic stresses and different hormones could regulate them. Akram *et al.* [17] reported that *Gossypium hirsutum* and *G. barbadense* stress-responsive *cis*-regulatory elements exceed the other identified elements. In turn, a more significant proportion of light-responsive elements was observed in *C. rosea*, corroborating these findings [24]. Considering these results, this information demonstrates the plasticity of the different roles that *NHX* genes can play during the growth and development of plants and between other numerous physiological processes.

It is estimated that the microRNAs (miRNAs) are small (20–24 nucleotides) non-coding RNA molecules that regulate gene expression by binding to target gene transcripts to inhibit their translation or promote mRNA degradation [71]. This study identified 22 miRNAs from five families targeting seven *PvNHX* genes (File S5). The

*PvNHX2*, *PvNHX4*, *PvNHX5*, *PvNHX8*, and *PvNHX9* genes were collectively targeted by PvumiRN2588. In addition, *PvNHX2* and *PvNHX7* were targeted by PvumiRN395. The miR395 family is an ancient and highly conserved miRNA family [72]. Previous studies showed that miR395 expression is important during stress since it controls sulfation-mediated hormonal activity [73]. Additionally, miR395 showed regulatory effects on plant salt stress tolerance [74]. Moreover, *PvNHX* genes were targeted by other miRNA families such as miR67, umiR56, and umiRN2597.

PvNHX2 primarily interacts with five proteins: SOS2, SOS3, AVP1, CBL1, and CBL10 (Fig. 6). SOS2 and SOS3 regulate intracellular $Na^+$ and $Ca^{2+}$ homeostasis by participating in the regulatory mechanism of salt stress. SOS1 is crucial in extruding harmful $Na^+$ from cells and is vital for plant salt tolerance. HKT1 imparts salt tolerance, while RCD1 protects chloroplasts from elevated ROS levels. HAK5, a high-affinity potassium transporter 5, plays a crucial role in the high-affinity potassium absorption noted in plant roots in saline circumstances [75]. Furthermore, calcineurin B-like (CBL) can engage with and regulate the CBL-interacting protein kinases (CIPKs) to facilitate $Ca^{2+}$ signal transduction. The genetic interaction between the CBL4 and CBL10 double mutant in Arabidopsis exhibited increased salt sensitivity compared with the cbl4 and cbl10 single mutants, indicating that CBL4 and CBL10 each regulate distinct salt-tolerance pathways [76]. We propose that these proteins and PvNHX proteins collaborate and participate in sodium ion transport across the membrane and the response to salt stress.

It is important to mention that the specificity of gene expression in different plant tissues and developmental stages provides essential information about the possible functions of genes. The various expression patterns displayed by the nine identified *PvNHX* genes and other analyses presented in this manuscript indicate that the modulation of these genes is differentiated in terms of the specific tissue and possibly the type of stress (Figs. 7,8). Previous research showed that one of the strategies of plants under salt stress is sequestering $Na^+$ to the vacuoles, alleviating $Na^+$ toxicity in the cytoplasm [77]. NHXs are crucial in sequestering $Na^+$ into vacuoles to maintain $Na^+$ homeostasis and improve plant salinity tolerance [78].

In this way, significant changes in the expression levels for the cultivar TR43477 (salt-susceptible) of some genes (*PvNHX2*, *3*, *6*, *7*, and *9*) in leaf tissues under salt-stress were observed (Fig. 8). We can speculate that the salt-tolerant cultivar Ispr showed an increased expression level for *PvNHX3* and *PvNHX8* genes in roots and leaves, respectively. *PvNHX3 and PvNHX8* are part of the Vac clade, suggesting that the NaCl-resistant mechanism of the common bean Ispr cultivar mainly involves the sequestration of $Na^+$ into vacuoles. Vac-class *NHXs* are essential for the salt tolerance of plants [22]. In *G. max*, *GmNHX* genes

demonstrated elevated expression levels in roots compared to shoots during salt stress [69]. Similar results were observed in *Zygophyllum xanthoxylum* [79] and *Puccinellia tenuiflora* [80]. The expression levels of the Vac *PvNHX8* gene in leaves in the Ispr cultivar (tolerant-salt) were significantly higher under salt stress, implying that *PvNHX8* can sequester Na$^+$ in leaves during salinity stress. The present study could be enhanced if further analysis were performed on physiological and molecular aspects in different tissues and responses to various abiotic stresses in the common bean.

This study provides conclusive evidence that the expression of some genes, such as *PvNHX2*, *4*, and *5* in roots, and *PvNHX1*, *4*, and *6*, was unaffected by salt stress, suggesting these genes may not contribute to the physiological responses associated with salt tolerance in *P. vulgaris* L. This indicates that this transcriptional diversity may be attributed to the genetic structures of the cultivars and the physical and chemical properties independent of NHX proteins. Therefore, by aiming to create a strategy that can mitigate the effects of climate change, this study shows that *in silico* analyses are relevant tools and contribute to identifying traits and genes related to stress salt in common beans.

## 5. Conclusions

The recent progress in plant genome-wide analyses has facilitated the identification and isolation of important genes and an evaluation of their roles in regulating yield and salt stress responses. This study identified nine putative *PvNHX* genes in the *P. vulgaris* L. genome. Phylogenetic analysis revealed that these *PvNHX* genes are grouped into two classes: Vac- (*PvNHX1*, *3*, *4*, *5*, *6*, *7*, *8*, and *9*) and PM-class NHXs (*PvNHX2*); meanwhile, the same clade motif compositions and exon/intron structures are conserved. Synteny event comparisons in the *NHX* genes in *P. vulgaris* L., *A. thaliana*, *O. sativa*, and *G. max* identified several orthologous genes. In addition, the synteny between *P. vulgaris* L. and *G. max* was conserved. The expression patterns differed across the various *P. vulgaris* L. tissues; *PvNHX7* and *PvNHX9* were the highest expressed genes in most analyzed tissues. The expression profiles of *PvNHX* genes in salt-tolerant (Ispir) and salt-susceptible (TR43477) genotypes of *P. vulgaris* L. revealed that some *PvNHX* genes were affected by salt stress. This study provided candidate genes for further functional research, which is essential for understanding the mechanism through which NHX genes regulate salt stress responses in *P. vulgaris*. Finally, to ensure food security and sustainable standard bean production worldwide, identifying new genes and varieties tolerant to saline stress will be extremely important for maintaining the yield and quality of this bean species in the future.

## Availability of Data and Materials

All data reported in this paper will also be shared by the corresponding author upon reasonable request.

## Author Contributions

EMB, and JO, performed *in silico* analysis and wrote the manuscript. TBS, conceived, provided technical support, and critical review. SGHS, conceived, provided technical support, and revised the manuscript. All authors contributed to editorial changes in the manuscript. All authors read and approved the final manuscript. All authors have participated sufficiently in the work and agreed to be accountable for all aspects of the work.

## Ethics Approval and Consent to Participate

Not applicable.

## Conflict of Interest

The authors declare no conflict of interest.

## Supplementary Material

Supplementary material associated with this article can be found, in the online version, at https://doi.org/10.31083/FBS26725.

## References

[1] Chaudhry S, Sidhu GPS. Climate change regulated abiotic stress mechanisms in plants: a comprehensive review. Plant Cell Reports. 2022; 41: 1–31. https://doi.org/10.1007/s00299-021-02759-5.

[2] İbrahimova U, Kumari P, Yadav S, Rastogi A, Antala M, Suleymanova Z, *et al*. Progress in understanding salt stress response in plants using biotechnological tools. Journal of Biotechnology. 2021; 329: 180–191. https://doi.org/10.1016/j.jbiotec.2021.02.007.

[3] Al Murad M, Khan AL, Muneer S. Silicon in Horticultural Crops: Cross-talk, Signaling, and Tolerance Mechanism under Salinity Stress. Plants (Basel, Switzerland). 2020; 9: 460. https://doi.org/10.3390/plants9040460.

[4] Haque MA, Rafii MY, Yusoff MM, Ali NS, Yusuff O, Datta DR, *et al*. Advanced breeding strategies and future perspectives of salinity tolerance in rice. Agronomy. 2021; 11: 1631. https://doi.org/10.3390/agronomy11081631.

[5] Dos Santos TB, Ribas AF, De Souza SGH, Budzinski IGF, Domingues DS. Physiological Responses to Drought, Salinity, and Heat Stress in Plants: A Review. Stresses. 2022; 2: 113–135. https://doi.org/10.3390/stresses2010009.

[6] van Zelm E, Zhang Y, Testerink C. Salt tolerance mechanisms of plants. Annual Review of Plant Biology. 2020; 71: 403–433. https://doi.org/10.1146/annurev-arplant-050718-100005.

[7] Hao S, Wang Y, Yan Y, Liu Y, Wang J, Chen S. A review on plant responses to salt stress and their mechanisms of salt resistance.

Horticulturae. 2021; 7: 132. https://doi.org/10.3390/horticultura e7060132.

[8] Karim R, Bouchra B, Fatima G, Filali-Maltouf A, Sbabou L. Plant NHX Antiporters: from function to biotechnological application with case study. Current Protein & Peptide Science. 2021; 22: 60–73. https://doi.org/10.2174/1389203721666201103085151.

[9] Brett CL, Tukaye DN, Mukherjee S, Rao R. The yeast endosomal Na$^+$ (K$^+$)/H$^+$ exchanger Nhx1 regulates cellular pH to control vesicle trafficking. Molecular Biology of the Cell. 2005; 16: 1396–1405. https://doi.org/10.1091/mbc.e04-11-0999.

[10] Wang Y, Ying J, Zhang Y, Xu L, Zhang W, Ni M, et al. Genome-wide identification and functional characterization of the cation proton antiporter (CPA) family related to salt stress response in radish (Raphanus sativus L.). International Journal of Molecular Sciences. 2020; 21: 8262. https://doi.org/10.3390/ijms21218262.

[11] Aharon GS, Apse, MP, Duan, S, Hua, X, Blumwald, E. Characterization of a family of vacuolar Na$^+$/H$^+$ antiporters in Arabidopsis thaliana. Plant and Soil. 2003; 253: 245–256. https://doi.org/10.1023/A:1024577205697.

[12] Pehlivan N, Sun L, Jarrett P, Yang X, Mishra N, Chen L, et al. Co-overexpressing a plasma membrane and a vacuolar membrane sodium/proton antiporter significantly improves salt tolerance in transgenic Arabidopsis plants. Plant and Cell Physiology. 2016; 57: 1069–1084. https://doi.org/10.1093/pcp/pcw055.

[13] Sharma H, Sharma A, Sidhu S, Upadhyay SK. Na$^+$/H$^+$ antiporter (NHX) and salt stress tolerance. In Upadhyay SK (ed.) Cation Transporters in Plants (pp. 99–113). Academic Press: Cambridge, Massachusetts, USA. 2022. https://doi.org/10.1016/B978-0-323-85790-1.00008-7.

[14] Bassil E, Zhang S, Gong H, Tajima H, Blumwald E. Cation Specificity of Vacuolar NHX-Type Cation/H$^+$ Antiporters. Plant Physiology. 2019; 179: 616–629. https://doi.org/10.1104/pp.18.01103.

[15] Chanroj S, Wang G, Venema K, Zhang MW, Delwiche CF, Sze H. Conserved and diversified gene families of monovalent cation/h(+) antiporters from algae to flowering plants. Frontiers in Plant Science. 2012; 3: 25. https://doi.org/10.3389/fpls.2012.00025.

[16] Sharma H, Taneja M, Upadhyay SK. Identification, characterization and expression profiling of cation-proton antiporter superfamily in Triticum aestivum L. and functional analysis of TaNHX4-B. Genomics. 2020; 112: 356–370. https://doi.org/10.1016/j.ygeno.2019.02.015.

[17] Akram U, Song Y, Liang C, Abid MA, Askari M, Myat AA, et al. Genome-Wide Characterization and Expression Analysis of NHX Gene Family under Salinity Stress in Gossypium barbadense and Its Comparison with Gossypium hirsutum. Genes. 2020; 11: 803. https://doi.org/10.3390/genes11070803.

[18] Dong J, Liu C, Wang Y, Zhao Y, Ge D, Yuan Z. Genome-wide identification of the NHX gene family in Punica granatum L. and their expressional patterns under salt stress. Agronomy. 2021; 11: 264. https://doi.org/10.3390/agronomy11020264.

[19] Solis CA, Yong MT, Zhou M, Venkataraman G, Shabala L, Holford P, et al. Evolutionary Significance of NHX Family and NHX1 in Salinity Stress Adaptation in the Genus Oryza. International Journal of Molecular Sciences. 2022; 23: 2092. https://doi.org/10.3390/ijms23042092.

[20] Gaxiola RA, Rao R, Sherman A, Grisafi P, Alper SL, Fink GR. The Arabidopsis thaliana proton transporters, AtNhx1 and Avp1, can function in cation detoxification in yeast. Proceedings of the National Academy of Sciences of the United States of America. 1999; 96: 1480–1485. https://doi.org/10.1073/pnas.96.4.1480.

[21] Fukuda A, Nakamura A, Hara N, Toki S, Tanaka Y. Molecular and functional analyses of rice NHX-type Na+/H+ antiporter genes. Planta. 2011; 233: 175–188. https://doi.org/10.1007/s00425-010-1289-4.

[22] Wu GQ, Wang JL, Li SJ. Genome-Wide Identification of Na$^+$/H$^+$ Antiporter (NHX) Genes in Sugar Beet (Beta vulgaris L.) and Their Regulated Expression under Salt Stress. Genes. 2019; 10: 401. https://doi.org/10.3390/genes10050401.

[23] Ayadi M, Martins V, Ben Ayed R, Jbir R, Feki M, Mzid R, et al. Genome Wide Identification, Molecular Characterization, and Gene Expression Analyses of Grapevine NHX Antiporters Suggest Their Involvement in Growth, Ripening, Seed Dormancy, and Stress Response. Biochemical Genetics. 2020; 58: 102–128. https://doi.org/10.1007/s10528-019-09930-4.

[24] Pu L, Lin R, Zou T, Wang Z, Zhang M, Jian S. Genome-Wide Identification, Primary Functional Characterization of the NHX Gene Family in Canavalia rosea, and Their Possible Roles for Adaptation to Tropical Coral Reefs. Genes. 2021; 13: 33. https://doi.org/10.3390/genes13010033.

[25] Huang L, Li Z, Sun C, Yin S, Wang B, Duan T, et al. Genome-wide identification, molecular characterization, and gene expression analyses of honeysuckle NHX antiporters suggest their involvement in salt stress adaptation. PeerJ. 2022; 10: e13214. https://doi.org/10.7717/peerj.13214.

[26] Asif MA, Zafar Y, Iqbal J, Iqbal MM, Rashid U, Ali GM, et al. Enhanced expression of AtNHX1, in transgenic groundnut (Arachis hypogaea L.) improves salt and drought tolerence. Molecular Biotechnology. 2011; 49: 250–256. https://doi.org/10.1007/s12033-011-9399-1.

[27] Yarra R, He SJ, Abbagani S, Ma B, Bulle M, Zhang WK. Overexpression of a wheat Na$^+$/H$^+$ antiporter gene (TaNHX2) enhances tolerance to salt stress in transgenic tomato plants (Solanum lycopersicum L.). Plant Cell Tissue Organ Culture. 2012; 111: 49–57. https://doi.org/10.1007/s11240-012-0169-y.

[28] Yarra R, Kirti PB. Expressing class I wheat NHX (TaNHX2) gene in eggplant (Solanum melongena L.) improves plant performance under saline condition. Functional & Integrative Genomics. 2019; 19: 541–554. https://doi.org/10.1007/s10142-019-00656-5.

[29] Brini F, Hanin M, Mezghani I, Berkowitz GA, Masmoudi K. Overexpression of wheat Na$^+$/H$^+$ antiporter TNHX1 and H$^+$−pyrophosphatase TVP1 improve salt- and drought-stress tolerance in Arabidopsis thaliana plants. Journal of Experimental Botany. 2007; 58: 301–308. https://doi.org/10.1093/jxb/erl251.

[30] Lu W, Guo C, Li X, Duan W, Ma C, Zhao M, et al. Overexpression of TaNHX3, a vacuolar Na$^+$/H$^+$ antiporter gene in wheat, enhances salt stress tolerance in tobacco by improving related physiological processes. Plant Physiology and Biochemistry. 2014; 76: 17–28. https://doi.org/10.1016/j.plaphy.2013.12.013.

[31] Yarra R. The wheat NHX gene family: potential role in improving salinity stress tolerance of plants. Plant Gene. 2019; 1: 100178. https://doi.org/10.1016/j.plgene.2019.100178.

[32] Wang B, Zhai H, He S, Zhang H, Ren Z, Zhang D, et al. A vacuolar Na$^+$/H$^+$, antiporter gene, IbNHX2, enhances salt and drought tolerance in transgenic sweetpotato. Scientia Horticulturae. 2016; 201: 153–166. https://doi.org/10.1016/j.scienta.2016.01.027.

[33] Bulle M, Yarra R, Abbagani S. Enhanced salinity stress tolerance in transgenic chilli pepper (Capsicum annuum L.) plants overexpressing the wheat antiporter (TaNHX2) gene. Molecular Breeding. 2016; 36: 36. https://doi.org/10.1007/s11032-016-0451-5.

[34] Dias PAS, Almeida DV, Melo PGS, Pereira HS, Melo LC. Effectiveness of breeding selection for grain quality in common bean. Crop Science. 2021; 61: 1127–1140. https://doi.org/10.1002/csc2.20422.

[35] Schmutz J, Mcclean PE, Mamidi S, Wu GA, Cannon SB,

Grimwood J, *et al.* Reference Genome for Common Bean and Genome-Wide Analysis of Dual Domestications. Nature Genetics. 2014; 46: 707–713. https://doi.org/10.1038/ng.3008.

[36] Goodstein DM, Shu S, Howson R, Neupane R, Hayes RD, Fazo J, *et al.* Phytozome: a comparative platform for green plant genomics. Nucleic Acids Research. 2012; 40: D1178–D1186. https://doi.org/10.1093/nar/gkr944.

[37] El-Gebali S, Mistry J, Bateman A, Eddy SR, Luciani A, Potter SC, *et al.* The Pfam protein families database in 2019. Nucleic Acids Research. 2019; 47: D427–D432. https://doi.org/10.1093/nar/gky995.

[38] Gasteiger E, Hoogland C, Gattiker A, Duvaud S, Wilkins MR, Appel RD, *et al.* Protein identification and analysis tools on the ExPASy Server. In Walker JM (ed.) The proteomics protocols handbook. Humana Press: Totowa. 2005. https://doi.org/10.1385/1-59259-584-7:531.

[39] Chou KC, Shen HB. Plant-mPLoc: a top-down strategy to augment the power for predicting plant protein subcellular localization. PloS One. 2010; 5: e11335. https://doi.org/10.1371/journal.pone.0011335.

[40] Krogh A, Larsson B, von Heijne G, Sonnhammer EL. Predicting transmembrane protein topology with a hidden Markov model: application to complete genomes. Journal of Molecular Biology. 2001; 305: 567–580. https://doi.org/10.1006/jmbi.2000.4315.

[41] Blom N, Gammeltoft S, Brunak S. Sequence and structure-based prediction of eukaryotic protein phosphorylation sites. Journal of Molecular Biology. 1999; 294: 1351–1362. https://doi.org/10.1006/jmbi.1999.3310.

[42] Hu B, Jin J, Guo AY, Zhang H, Luo J, Gao G. GSDS 2.0: an upgraded gene feature visualization server. Bioinformatics (Oxford, England). 2015; 31: 1296–1297. https://doi.org/10.1093/bioinformatics/btu817.

[43] Bailey TL, Johnson J, Grant CE, Noble WS. The MEME Suite. Nucleic Acids Research. 2015; 43: W39–W49. https://doi.org/10.1093/nar/gkv416.

[44] Voorrips RE. MapChart: software for the graphical presentation of linkage maps and QTLs. The Journal of Heredity. 2002; 93: 77–78. https://doi.org/10.1093/jhered/93.1.77.

[45] Zhang Z, Li J, Zhao XQ, Wang J, Wong GKS, Yu J. KaKs_Calculator: calculating Ka and Ks through model selection and model averaging. Genomics, Proteomics & Bioinformatics. 2006; 4: 259–263. https://doi.org/10.1016/S1672-0229(07)60007-2.

[46] Kumar S, Stecher G, Li M, Knyaz C, Tamura K. MEGA X: Molecular Evolutionary Genetics Analysis across Computing Platforms. Molecular Biology and Evolution. 2018; 35: 1547–1549. https://doi.org/10.1093/molbev/msy096.

[47] Huang Z, Zhong XJ, He J, Jin SH, Guo HD, Yu XF, *et al.* Genome-Wide Identification, Characterization, and Stress-Responsive Expression Profiling of Genes Encoding LEA (Late Embryogenesis Abundant) Proteins in Moso Bamboo (Phyllostachys edulis). PloS One. 2016; 11: e0165953. https://doi.org/10.1371/journal.pone.0165953.

[48] Lescot M, Déhais P, Thijs G, Marchal K, Moreau Y, Van de Peer Y, *et al.* PlantCARE, a database of plant cis-acting regulatory elements and a portal to tools for in silico analysis of promoter sequences. Nucleic Acids Research. 2002; 30: 325–327. https://doi.org/10.1093/nar/30.1.325.

[49] Kelley LA, Mezulis S, Yates CM, Wass MN, Sternberg MJE. The Phyre2 web portal for protein modeling, prediction and analysis. Nature Protocols. 2015; 10: 845–858. https://doi.org/10.1038/nprot.2015.053.

[50] Metsalu T, Vilo J. ClustVis: a web tool for visualizing clustering of multivariate data using Principal Component Analysis and heatmap. Nucleic Acids Research. 2015; 43: W566–W570. https://doi.org/10.1093/nar/gkv468.

[51] Niron H, Barlas N, Salih B, Türet M. Comparative Transcriptome, Metabolome, and Ionome Analysis of Two Contrasting Common Bean Genotypes in Saline Conditions. Frontiers in Plant Science. 2020; 11: 599501. https://doi.org/10.3389/fpls.2020.599501.

[52] Jabeen Z, Irshad F, Hussain N, Han Y, Zhang G. NHX-Type $Na^+/H^+$ Antiporter Gene Expression Under Different Salt Levels and Allelic Diversity of *HvNHX* in Wild and Cultivated Barleys. Frontiers in Genetics. 2022; 12: 809988. https://doi.org/10.3389/fgene.2021.809988.

[53] Cao B, Long D, Zhang M, Liu C, Xiang Z, Zhao A. Molecular characterization and expression analysis of the mulberry Na(+)/H(+) exchanger gene family. Plant Physiology and Biochemistry: PPB. 2016; 99: 49–58. https://doi.org/10.1016/j.plaphy.2015.12.010.

[54] Khare T, Joshi S, Kaur K, Srivastav A, Shriram V, Srivastava AK, *et al.* Genome-wide *in silico* identification and characterization of sodium-proton ($Na^+/H^+$) antiporters in Indica rice. Plant Gene. 2021; 26: 100280. https://doi.org/10.1016/j.plgene.2021.100280.

[55] Paul A, Chatterjee A, Subrahmanya S, Shen G, Mishra N. NHX Gene Family in *Camellia sinensis*: *In-silico* Genome-Wide Identification Expression Profiles and Regulatory Network Analysis. Frontiers in Plant Science. 2021; 12: 777884. https://doi.org/10.3389/fpls.2021.777884.

[56] Ayadi M, Ben Ayed R, Mzid R, Aifa S, Hanana M. Computational approach for structural feature determination of grapevine NHX antiporters. BioMed Research International. 2019; 2019: 1031839. https://doi.org/10.1155/2019/1031839.

[57] Pardo JM, Cubero B, Leidi EO, Quintero FJ. Alkali cation exchangers: roles in cellular homeostasis and stress tolerance. Journal of Experimental Botany. 2006; 57: 1181–1199. https://doi.org/10.1093/jxb/erj114.

[58] Barragan V, Leidi EO, Andres Z, Rubio L, De Luca A, Fernandez JA, *et al.* Ion exchangers NHX1 and NHX2 mediate active potassium uptake into vacuoles to regulate cell turgor and stomatal function in Arabidopsis. The Plant Cell. 2012; 24: 1127–1142. https://doi.org/10.1105/tpc.111.095273.

[59] Huang Y, Guan C, Liu Y, Chen B, Yuan S, Cui X, *et al.* Enhanced Growth Performance and Salinity Tolerance in Transgenic Switchgrass via Overexpressing Vacuolar $Na^+$ $(K^+)/H^+$ Antiporter Gene (*PvNHX1*). Frontiers in Plant Science. 2017; 8: 458. https://doi.org/10.3389/fpls.2017.00458.

[60] Koralewski TE, Krutovsky KV. Evolution of exon-intron structure and alternative splicing. PloS One. 2011; 6: e18055. https://doi.org/10.1371/journal.pone.0018055.

[61] Liu J, Liu J, Wang H, Khan A, Xu Y, Hou Y, *et al.* Genome wide identification of GDSL gene family explores a novel GhirGDSL26 gene enhancing drought stress tolerance in cotton. BMC Plant Biology. 2023; 23: 14. https://doi.org/10.1186/s12870-022-04001-0.

[62] Zaheer M, Rehman SU, Khan SH, Shahid S, Rasheed A, Naz R, *et al.* Characterization of new COBRA like (COBL) genes in wheat (Triticum aestivum) and their expression analysis under drought stress. Molecular Biology Reports. 2022; 49: 1379–1387. https://doi.org/10.1007/s11033-021-06971-0.

[63] Tian F, Chang E, Li Y, Sun P, Hu J, Zhang J. Expression and integrated network analyses revealed functional divergence of NHX-type $Na^+/H^+$ exchanger genes in poplar. Scientific Reports. 2017; 7: 2607. https://doi.org/10.1038/s41598-017-02894-8.

[64] Ahmad B, Zhang S, Yao J, Rahman MU, Hanif M, Zhu Y, *et al.* Genomic Organization of the B3-Domain Transcription Factor Family in Grapevine (*Vitis vinifera* L.) and Expression during Seed Development in Seedless and Seeded Cultivars. International Journal of Molecular Sciences. 2019; 20: 4553.

https://doi.org/10.3390/ijms20184553.

[65] Kong H, Landherr LL, Frohlich MW, Leebens-Mack J, Ma H, dePamphilis CW. Patterns of gene duplication in the plant SKP1 gene family in angiosperms: evidence for multiple mechanisms of rapid gene birth. The Plant Journal: for Cell and Molecular Biology. 2007; 50: 873–885. https://doi.org/10.1111/j.1365-313X.2007.03097.x.

[66] Liu X, Li D, Zhang S, Xu Y, Zhang Z. Genome-wide characterization of the rose (Rosa chinensis) WRKY family and role of RcWRKY41 in gray mold resistance. BMC Plant Biology. 2019; 19: 522. https://doi.org/10.1186/s12870-019-2139-6.

[67] Chen HT, Chen X, Wu BY, Yuan XX, Zhang HM, Cui XY, *et al.* Whole-genome identification and expression analysis of $K^+$ efflux antiporter (KEA) and $Na^+/H^+$ antiporter (NHX) families under abiotic stress in soybean. Journal of Integrative Agriculture, 2015; 14: 1171–1183. https://doi.org/10.1016/S2095-3119(14)60918-7.

[68] Hima Kumari P, Anil Kumar S, Ramesh K, Sudhakar Reddy P, Nagaraju M, Bhanu Prakash A, *et al*. Genome-Wide Identification and Analysis of *Arabidopsis* Sodium Proton Antiporter (NHX) and Human Sodium Proton Exchanger (NHE) Homologs in *Sorghum bicolor*. Genes. 2018; 9: 236. https://doi.org/10.3390/genes9050236.

[69] Joshi S, Kaur K, Khare T, Srivastava AK, Suprasanna P, Kumar V. Genome-wide identification, characterization and transcriptional profiling of NHX-type ($Na^+/H^+$) antiporters under salinity stress in soybean. 3 Biotech. 2021; 11: 16. https://doi.org/10.1007/s13205-020-02555-0.

[70] Schmitz RJ, Grotewold E, Stam M. Cis-regulatory sequences in plants: Their importance, discovery, and future challenges. The Plant Cell. 2022; 34: 718–741. https://doi.org/10.1093/plcell/koab281.

[71] Su W, Raza A, Gao A, Jia Z, Zhang Y, Hussain MA, *et al*. Genome-Wide Analysis and Expression Profile of Superoxide Dismutase (SOD) Gene Family in Rapeseed (*Brassica napus* L.) under Different Hormones and Abiotic Stress Conditions. Antioxidants (Basel, Switzerland). 2021; 10: 1182. https://doi.org/10.3390/antiox10081182.

[72] Gao Z, Ma C, Zheng C, Yao Y, Du Y. Advances in the regulation of plant salt-stress tolerance by miRNA. Molecular Biology Reports. 2022; 49: 5041–5055. https://doi.org/10.1007/s11033-022-07179-6.

[73] Kopriva S, Mugford SG, Baraniecka P, Lee BR, Matthewman CA, Koprivova A. Control of sulfur partitioning between primary and secondary metabolism in Arabidopsis. Frontiers in Plant Science. 2012; 3: 163. https://doi.org/10.3389/fpls.2012.00163.

[74] Ding D, Zhang L, Wang H, Liu Z, Zhang Z, Zheng Y. Differential expression of miRNAs in response to salt stress in maize roots. Annals of Botany. 2009; 103: 29–38. https://doi.org/10.1093/aob/mcn205.

[75] Li SJ, Wu GQ, Lin LY. AKT1 HAK5 SKOR HKT1,5 SOS1 and NHX1 synergistically control $Na^+$ and $K^+$ homeostasis in sugar beet (*Beta vulgaris* L.) seedlings under saline conditions. Journal of Plant Biochemistry and Biotechnology. 2022; 31: 71–84. https://doi.org/10.1007/s13562-021-00656-2.

[76] Yang Y, Zhang C, Tang RJ, Xu HX, Lan WZ, Zhao F, *et al.* Calcineurin B-Like proteins CBL4 and CBL10 mediate two independent salt tolerance pathways in *Arabidopsis*. International Journal of Molecular Sciences. 2019; 20: 2421. https://doi.org/10.3390/ijms20102421.

[77] Meng K, Wu Y. Footprints of divergent evolution in two $Na^+/H^+$ type antiporter gene families *NHX* and *SOS1*) in the genus *Populus*. Tree Physiology. 2018; 38: 813–824. https://doi.org/10.1093/treephys/tpx173.

[78] Li N, Wang X, Ma B, Du C, Zheng L, Wang Y. Expression of a $Na^+/H^+$ antiporter *RtNHX1* from a recretohalophyte *Reaumuria trigyna* improved salt tolerance of transgenic *Arabidopsis thaliana*. Journal of Plant Physiology. 2017; 218: 109–120. https://doi.org/10.1016/j.jplph.2017.07.015.

[79] Ma Q, Bao AK, Chai WW, Wang WY, Zhang JL, Li YX, *et al.* Transcriptomic analysis of the succulent xerophyte *Zygophyllum xanthoxylum* in response to salt treatment and osmotic stress. Plant and Soil. 2016; 402: 343–361. http://www.jstor.org/stable/43872780.

[80] Zhang WD, Wang P, Bao Z, Ma Q, Duan LJ, Bao AK, *et al.* SOS1, HKT1;5, and NHX1 synergistically modulate $Na^+$ homeostasis in the halophytic grass *Puccinellia tenuiflora*. Frontiers in Plant Science. 2017; 8: 576. https://doi.org/10.3389/fpls.2017.00576.